Solution NMR Study of Methyltin(IV)-Cupferronates: Analysis of a Unique Dismutation Reaction and Preorganization Process

Gábor Tárkányi* and Andrea Deák

Institute of Structural Chemistry, Chemical Research Center of the Hungarian Academy of Sciences, Pusztaszeri út 59-67, H-1025 Budapest, Hungary

Received April 12, 2005

Multinuclear multidimensional ^{1}H, ^{13}C, and ^{119}Sn NMR data indicated that both the cyclic tetrameric $[Me_3Sn(ON(NO)Ph)]_4$ ($\mathbf{1}_t$) and dimeric $[Me_2Sn(ON(NO)Ph)_2]_2$ ($\mathbf{2}_d$) supramolecules are predominantly monomeric $[Me_3Sn(ON(NO)Ph)]_1$ ($\mathbf{1}_m$) and $[Me_2Sn(ON(NO)Ph)_2]_1$ ($\mathbf{2}_m$) in noncoordinating solvents ($CDCl_3$, CD_2Cl_2) at room temperature. This has been proven by the concerted interpretation of (1) Me−Sn−Me angles calculated from *J*-coupling data; (2) tin coordination numbers deduced from ^{119}Sn chemical shift data; and (3) molecular hydrodynamic radii calculated from the measurement of translational diffusion constants. Both $\mathbf{1}_m$ and $\mathbf{2}_m$ monomers underwent a *cis*−*trans* conformational exchange that is fast on the chemical shift time scales. In noncoordinating solvents the dominance of the *cis*-TBP and *cis*-O_h conformations was characteristic for $\mathbf{1}_m$ and $\mathbf{2}_m$, respectively. In coordinating solvents (DMSO, pyridine, methanol), the *trans*-conformers dominated and the formation of specific solute−solvent $\mathbf{1}_m$* and $\mathbf{2}_m$* coordination complexes was confirmed. The solvent-induced *cis*−*trans* conformational exchange was held responsible for the demethylation reaction of $\mathbf{1}_m$, which yielded $\mathbf{2}_m$ and the byproduct Me_4Sn. ^{1}H NMR kinetic experiments have proven that the dismutation process followed a second-order 2 A → B + C type kinetics. In Lewis base solvents, the dismutation product $\mathbf{2}_m$ was stabilized by the formation of a heptacoordinated solute−solvent complex $\mathbf{2}_m$*, which then underwent no further dismutation. The stability constant of the pyridine complex of $\mathbf{2}_m$ was determined from the analysis of NMR titration data. The mechanism of the methyl-migrational process was proposed on the basis of solvent-induced $\mathbf{1}_m$ (*cis*) ⇌ $\mathbf{1}_m$* (*trans*) conformational equilibrium. Low-temperature ^{1}H and ^{119}Sn NMR experiments in noncoordinating solvents revealed the first example of a $\mathbf{1}_m$ ⇌ $\mathbf{1}_t$ preorganization process leading to the re-formation of a solvated 20-membered macrocycle ($\mathbf{1}_t$).

Introduction

We have previously reported the preparation, X-ray structural determination, and basic NMR characterization of two supramolecular methyltin(IV)-*N*-nitroso-*N*-phenylhydroxylaminato (−cupferronato, −ON(NO)Ph) complexes: $[Me_3Sn(ON(NO)Ph)]_4$ ($\mathbf{1}_t$) and $[Me_2Sn(ON(NO)Ph)_2]_2$ ($\mathbf{2}_d$) (see Chart 1).[1,2] It was observed that the crystallization of the cyclic tetramer $\mathbf{1}_t$ from methanol yielded dimeric $\mathbf{2}_d$. Additionally we have also seen that the reaction of both $\mathbf{1}_t$ and $\mathbf{2}_d$ with N-donor ligands (such as pyridine and 4,4′-bipyridine) gave identical products.[2,3] We have deduced that the process behind the $\mathbf{1}_t$ → $\mathbf{2}_d$ transformation is a methyl-migrational dismutation reaction.[3] Similar dismutations in organometallic chemistry may provide alternative synthetic routes, but they are also potential sources of sample instability, preventing the preparation of devised structures via recrystallization.[4,5] Such methyl-migrational processes received scant attention in the literature, and the spectroscopic studies devoted to this area are fragmented.[6−8] This led us to investigate the so far uncharacterized nature of the dismutation reaction of $\mathbf{1}_t$ by solution NMR spectroscopy. We carried out kinetic experiments in the NMR spectrometer to prove our previous deduction concerning the reaction mechanism: the appearance of the byproduct Me_4Sn:

$$\mathbf{1}_t \rightarrow \mathbf{2}_d + 2\ Me_4Sn$$

We also aimed to clarify whether compounds $\mathbf{1}_t$ and $\mathbf{2}_d$ retain their self-assembled structures in the liquid phase at room temperature or constitute predominantly monomeric solvates. However, in contrast to the solid state the evidence for the Sn−O bond formation in

(1) Deák, A.; Haiduc, I.; Párkányi, L.; Venter, M.; Kálmán, A. *Eur. J. Inorg. Chem.* **1999**, 1593−1596.
(2) Deák, A.; Venter, M.; Kálmán, A.; Párkányi, L.; Radics, L.; Haiduc, I. *Eur. J. Inorg. Chem.* **2000**, 127−132.
(3) Deák, A.; Radics, L.; Kálmán, A.; Párkányi, L.; Haiduc, I. *Eur. J. Inorg. Chem.* **2001**, 2849−2856.
(4) Gielen, M.; De Clercq, M.; De Poorter, B. *J. Organomet. Chem.* **1972**, *34*, 305−313.
(5) Bancroft, G. M.; Davies, B. W.; Payne, N. C.; Sham, T. K. *J. Chem. Soc., Dalton* **1975**, 973−978.
(6) Eujen, R.; Jahn, N. *J. Fluor. Chem.* **1995**, *71*, 75−79.
(7) Craig, P. J.; Rapsomanikis, S. *Inorg. Chim. Acta* **1983**, *80*, L19−L21.
(8) Komura, M.; Tanaka, T.; Okawara, R. *Inorg. Chim. Acta* **1968**, *2*, 321−324.

10.1021/om050279y CCC: $30.25
Publication on Web 06/23/2005

Chart 1

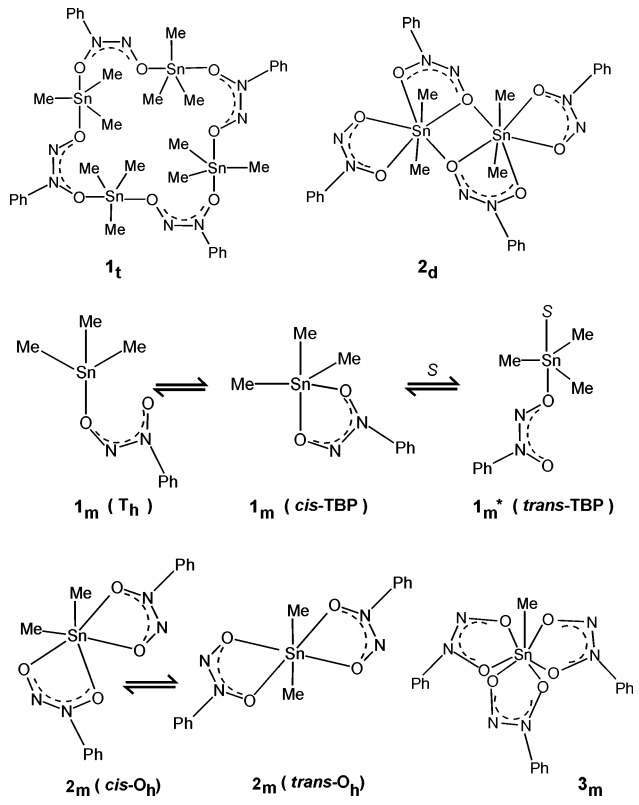

solution often remains encoded in averaged NMR parameters due to the various dynamic (e.g., internal motion, chemical exchange) processes at room temperature.[9] We expected from our previous experience that the interaction of organotin(IV) compounds with coordinating solvent molecules can interfere with the network of solute−solute association equilibria. When some of these processes induce specific solute−solute interactions, this leads to ligand exchange reactions. Despite years of spectroscopic studies in organotin chemistry, the tendency of organotin(IV) compounds to form solvated self-associated complexes still makes the characterization of their solution structures far from straightforward.

We report a summary of solution NMR results after dissolving the structurally well-defined crystals $\mathbf{1}_t$ and $\mathbf{2}_d$ in various solvents. Kinetic, temperature-dependent, and tin-based titration measurements[10] not yet published for the above family of compounds are presented. Diffusion ordered spectroscopy (DOSY) is utilized for the characterization of the self-diffusion behavior of methyltin(IV)-cupferronate solvates. Being inversely proportional to the hydrodynamic radius, the diffusion constant is an important molecular property in the identification of dissolved supramolecular organometallic species.[11−13]

(9) Pons, M.; Millet, O. *Prog. Nucl. Magn. Reson.* **2001**, *38*, 267−324.
(10) Tsagatakis, J. K.; Chaniotakis, N. A.; Jurkschat, K.; Damoun, S.; Geerlings, P.; Bouhdid, A.; Gielen, M.; Verbruggen, I.; Biesemans, M.; Martins, J. C.; Willem, R. *Helv. Chim. Acta* **1999**, *82*, 531−542.
(11) Valentini, M.; Pregosin, P. S.; Ruegger, H. *Organometallics* **2000**, *19*, 2551−2555.
(12) Zuccaccia, C.; Bellachioma, G.; Cardaci, G.; Macchioni, A. *Organometallics* **2000**, *19*, 4663−4665.
(13) Ribot, F.; Escax, V.; Martins, J. C.; Biesemans, M.; Ghys, L.; Verbruggen, I.; Willem, R. *Chem. Eur. J.* **2004**, *10*, 1747−1751.

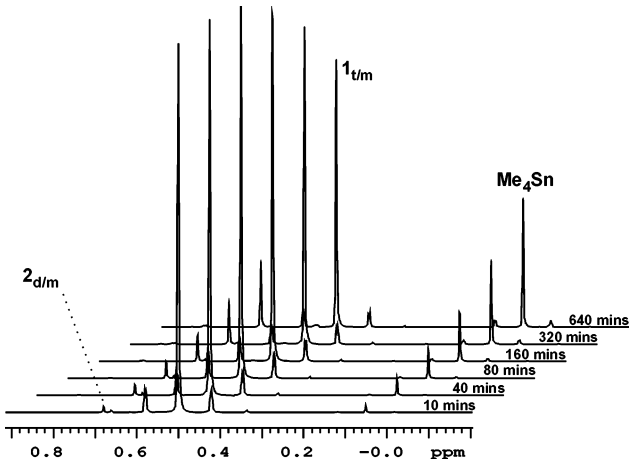

Figure 1. ^{1}H NMR kinetic study in methanol-d_4 at 25 °C. Spectra were acquired shortly after the dissolution of the $\mathbf{1}_t$ crystals in 0.75 mL of solvent (0.46 M for $\mathbf{1}_m$). The relative time spacings are indicated.

Results and Discussion

Investigation of the Dismutation Kinetics. Figure 1. shows the time-dependent ^{1}H NMR spectra of $\mathbf{1}_t$ shortly after dissolution of the crystals in methanol. The dismutation reaction proceeded spontaneously at room temperature, yielding a mixture of Me_4Sn and solvated $\mathbf{2}_d$. The reaction participants were identified both by standard additions and by various spectroscopic means (see later). The integral ratio of the newly formed methyl moieties remained Me_2Sn:Me_4Sn = 1:2 at each data point up to 50% conversion. This observation has verified our previous assumption that the methanol solvation of $\mathbf{1}_t$ is accompanied by a mutual methyl group migration between two central tin atoms, preventing the preparation of $\mathbf{1}_t$ via recrystallization from said solvent. Little is known about the exact mechanism of this dismutation process. The concentration change of dissolved $\mathbf{1}_t$ recorded by the appropriate Me_3Sn integrals as a function of time revealed second-order kinetics. The simplified kinetic equation that describes the system in agreement with the measured stoichiometry of the methyl protons is

$$2\,A \rightarrow B + C \qquad (1)$$

In other words when the dissolved species $\mathbf{1}_t$ and $\mathbf{2}_d$ are formally expressed in terms of the corresponding monomers, 2 [$\mathbf{1}_m$] → [$\mathbf{2}_m$] + [Me_4Sn] holds for the measured NMR integral ratios. Accordingly the 1/[*A*] vs *t* representation in Figure 2 provided a linear fit, and the rate constant k ($L \cdot mol^{-1} \cdot s^{-1}$) could be determined from the slope (at $[A]_0 = 0.46$ mol/L). The numeric results of the kinetics measured in five different solvents using the same initial concentrations are compared in Table 1. It was found that stronger Lewis base solvents (C_5D_5N, DMSO) induced dismutation at markedly faster rates than methanol, while the process was two magnitudes slower in acetone-d_6 and nearly infinitely slow in a nonpolarizing solvent, $CDCl_3$. In the latter, radical photodegradation of the cupferronato moiety accompanied by the appearance of subsequent degradation products prevented us from measuring the reaction rates for more than 2 days.

Solvent Effect and Oligomerization Equilibria. Since the reaction rates were influenced by the coordi-

Table 1. Dependence of the Rate of Reaction k on the Choice of the Solvent for the Dismutation of $\mathbf{1}_{t/m}$ (0.46 M for $\mathbf{1}_m$)

	$CDCl_3$	acetone	methanol	pyridine	DMSO
k ($L \cdot mol^{-1} \cdot s^{-1}$)	$3.38 \times 10^{-7} \pm 3.7 \times 10^{-9}$	$2.97 \times 10^{-5} \pm 4.5 \times 10^{-8}$	$6.98 \times 10^{-5} \pm 1.3 \times 10^{-7}$	$9.03 \times 10^{-5} \pm 5.4 \times 10^{-8}$	

Table 2. Chemical Shift $\delta(^{119}Sn)$ and J-Coupling [$^2J(^{119}Sn-^1H)$, $^1J(^{119}Sn-^{13}C)$] Data of Methyltin(IV)-Cupferronates $\mathbf{1}_t$, $\mathbf{2}_d$, and $\mathbf{3}_m$ Dissolved in Various Solvents (30 mM for the monomers)[a]

		solvent				
NMR parameter	compound	$CDCl_3$	acetone	methanol	pyridine	DMSO
δ_{Sn119} (ppm)	$\mathbf{1}_{m/t}$	+114.0	+100.0	+58.1	+32.4	+19.1
	$\mathbf{2}_{m/d}$	−159.1	−166.9	−316.6	−367.7	−361.4
	$\mathbf{3}_m$	−478.6	−478.0	−479.3	−474.1	−474.6
$\lvert^2J_{1H-119Sn}\rvert$ (Hz)	$\mathbf{1}_{m/t}$	54.8	58.0	64.6	63.2	61.2
	$\mathbf{2}_{m/d}$	76.8	79.3	108.4	112.0	115.2
	$\mathbf{3}_m$	125.3	125.9	124.9	124.2	123.4
$\lvert^1J_{13C-119Sn}\rvert$ (Hz)	$\mathbf{1}_{m/t}$	405	425	481	482	509
	$\mathbf{2}_{m/d}$	660	679	1029	1119	1118
	$\mathbf{3}_m$	1178	1186	1187	1174	1163

[a] Indexes refer to the possible equilibrium between monomeric/oligomeric states.

nating strength of the solvent, we attempted to find the spectral differences between measurements in coordinating and noncoordinating solvents that could rationalize this correlation. Because the stoichiometry of the dismutation reaction is such that it allows the interpretation of the mechanism on the basis of intramolecular rearrangements within the tetrameric species $\mathbf{1}_t$, it raised the question whether compounds $\mathbf{1}_t$ and $\mathbf{2}_d$ exist as stable symmetric self-associates or are predominantly monomeric ($\mathbf{1}_m$ and $\mathbf{2}_m$) in solution. Answering this requires some circumspection due to the presence of $[\mathbf{1}_t] \equiv [\mathbf{1}_m]_4 \rightleftharpoons 4\ [\mathbf{1}_m]$ and/or $[\mathbf{2}_d] \equiv [\mathbf{2}_m]_2 \rightleftharpoons 2\ [\mathbf{2}_m]$ equilibria in solution. Initially, it is unspecified whether these equilibria are fast on the chemical shift time scales (^1H, ^{13}C, ^{119}Sn) or are shifted toward either species: monomeric or oligomeric. In both extreme cases one set of resonances are detected due to the symmetric nature of the supramolecules. However when the equilibria are shifted by concentration and temperature changes or by the presence of complexing ligands (e.g., coordinating solvents), the dynamic nature of the various solute−solute and solute−solvent complexation processes can be fully characterized. These experimental results will be presented in the following.

Analysis of the ^{119}Sn Chemical Shifts. We extend here our structural study of methyltin(IV)-cupferronates by the synthesis and characterization of a third compound in the row: the monomethyltin(IV) derivative, $[MeSn(ON(NO)Ph)_3]_1$ ($\mathbf{3}_m$) (Chart 1). The room-temperature spectroscopic properties of compounds $\mathbf{1}_t$, $\mathbf{2}_d$, and $\mathbf{3}_m$ dissolved in various solvents are collected in Table 2. The ^{119}Sn chemical shifts for $CDCl_3$-solvated $\mathbf{1}_t$ (+114.0 ppm) and $\mathbf{2}_d$ (−159.1 ppm) lie at an intermediate region for tin coordination numbers CN = 4 or 5 and CN = 5 or 6, respectively.[14] Given that the bidentate cupferronato anion has the tendency to show not only five-membered chelating but also bridging- and bimetallic bridging-chelating coordination patterns, in principle we face the problem that the dynamic equilibrium of all four coordination types (including the monodentate) may add its contribution to the observed ^{119}Sn chemical shift in solution. Therefore ^{119}Sn chemical shift data alone are insufficient for the unambiguous determination of organotin coordination geometries without prior knowledge about the complexation dynamics. Nevertheless, on the basis of the literature data for other five-membered organotin-chelates[15] (such as maltolates,[16] tropolonates[17−19]) it can be said that the ^{119}Sn shift value of $\mathbf{2}_d$ in $CDCl_3$ contradicts with a heptacoordinated state of the tin that was characteristic for its crystal structure. The CN = 6 for compound $\mathbf{2}_d$ and CN = 7 for compound $\mathbf{3}_m$ can be rationalized according to analogy with tropolonates provided that both are monomeric in solution. The ^{119}Sn chemical shift for dissolved $\mathbf{1}_t$ is acceptable for the predominance of a pentacoordinated *cis*-trigonal bipyramid (TBP) conformation of a monomer ($\mathbf{1}_m$) (see Chart 1), but the possibility for the formation of a symmetrical pentacoordinated macrocycle ($\mathbf{1}_t$) in equilibrium with a monomeric monodendate distorted tetrahedron (T_h) is also a plausible explanation at this point.

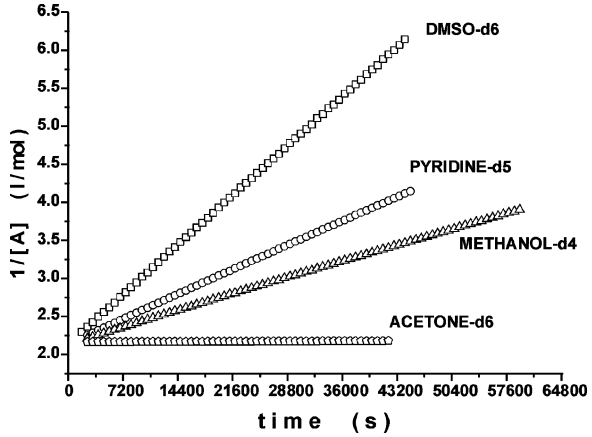

Figure 2. $1/[A]$ vs t representation of the second-order dismutation kinetics of dissolved $\mathbf{1}_t$ in various solvents (25 °C, $[A]_0 = 0.46$ mol/L for $\mathbf{1}_m$).

(14) Nádvorník, M.; Holeèek, J.; Handlíø, K. *J. Organomet. Chem.* **1984**, *275*, 43−51.

(15) Otera, J.; Hinoishi, T.; Kawabe, Y.; Okawara, R. *Chem. Lett.* **1981** 273−274.

(16) Bhattacharya, S.; Seth, N.; Gupta, V. D.; Nöth, H.; Polborn, K.; Thomann, M.; Schwenk, H. *Chem. Ber.* **1994**, *192*, 1895−1900.

(17) Otera, J. *J. Organomet. Chem.* **1981**, *221*, 57−61.

(18) Otera, J.; Kusaba, A.; Hinoishi, T.; Kawasaki, Y. *J. Organomet. Chem.* **1982**, *228*, 223−228.

(19) Camacho-Camacho, C.; Contreras, R.; Nöth, H.; Bechmann, M.; Sebald, S.; Milius, W.; Wrackmeyer, B. *Magn. Reson. Chem.* **2002**, *40*, 31−40.

Table 3. Calculated Me−Sn−Me Bond Angles (deg), Calculated from $^2J(^{119}Sn-^1H)$[a] and $^1J(^{119}Sn-^{13}C)$[b] *J*-Coupling Data

Me−Sn−Me	compound	$CDCl_3$	acetone	methanol	pyridine	DMSO
calcd from	$\mathbf{1}_{m/t}$	109.4	111.0	115.3	114.3	112.9
$^2J(^{119}Sn-^1H)$	$\mathbf{2}_{m/d}$	127.0	130.0	179.5	187.5	195.0
calcd from	$\mathbf{1}_{m/t}$	110.6	112.4	117.7	117.7	120.3
$^1J(^{119}Sn-^{13}C)$	$\mathbf{2}_{m/d}$	134.4	136.2	168.9	177.3	177.2

[a] Refers to ref 23 in text. [b] Refers to ref 24 in text.

Both $\mathbf{1}_t$ and $\mathbf{2}_d$ experienced significantly large upfield ^{119}Sn shifts when dissolved in coordinating solvents, suggesting higher coordination numbers around the central tin atoms. This observation is in agreement with the faster dismutation rates of $\mathbf{1}_t$ found in Lewis base solvents, but no further dismutation of $\mathbf{2}_d$ was experienced. Since the ^{119}Sn shifts of $\mathbf{3}_m$ were unaffected by the coordinating strength of the solvent, the hypothesis about its predominantly monomeric state in solution seems reasonable.

Analysis of the *J* Coupling Constants. Additional structural characterization of the dissolved compounds $\mathbf{1}_t$, $\mathbf{2}_d$, and $\mathbf{3}_m$ was possible from the analysis of their relevant one- $^1J(^{119}Sn-^{13}C)$ (^1J) and two-bond $^2J(^{119}Sn-^1H)$ (^2J) scalar coupling constants.[20] The experimental values determined in various solvents are collected in Table 3. Lockhart et al. have determined from solid-state NMR[21] that the $|^1J|$ and $|^2J|$ absolute values of these coupling constants can be used to estimate the Me−Sn−Me bond angles with reasonably good accuracy.[22,23] Their theory was extended to solution NMR as well with a notice that depending on the nature of the chelating ligands the Me−Sn−Me angles may differ significantly whether determined from the $|^1J|$ or $|^2J|$ values.[24] For solvated $\mathbf{2}_d$ we experienced a minor but similar discrepancy, as the bond angles became 134.6° ($|^1J|$) vs 127.0° ($|^2J|$) in $CDCl_3$ (see Table 3). If $\mathbf{2}_d$ were predominantly monomeric ($\mathbf{2}_m$) in solution, a possible explanation for this would be a *cis*-octahedral (*cis*-O_h) conformation around the central tin. Our in vacuo PM3 semiempirical calculations reinforced this, as the equilibrium geometry for the monomeric *cis* conformer was ca. 17 kJ/mol lower in potential energy than the corresponding *trans*-octahedral (*trans*-O_h) one (Chart 1). For compound $\mathbf{1}_t$ the approximate bond angle 113° ($|^2J|$) in $CDCl_3$ contradicted the *trans*-trigonal bipyramydal (*trans*-TBP) geometry necessary for the macrocyclic organization and provided further evidence for its monomeric nature.

The $|^1J|$ and $|^2J|$ coupling constants of dissolved $\mathbf{1}_t$ and $\mathbf{2}_d$ increased with the coordinating strength of the solvents and therefore yielded larger Me−Sn−Me bond angle values (see Table 4). In DMSO the corresponding Me−Sn−Me bond angles reached the characteristic solid-state values ~120° ($\mathbf{1}_t$) and ~180° ($\mathbf{2}_d$), for which solute−solvent complexation of the presumably monomeric forms $\mathbf{1}_m$ and $\mathbf{2}_m$ is envisaged. Based on $|^2J|$ the *trans*-O_h conformation has been suggested earlier for the bis(kojato)dimethyltin(IV) complex in DMSO although without consideration of a solvent coordination model.[25] The $|^1J|$ and $|^2J|$ values for $\mathbf{3}_m$ were completely unaffected by the coordinating strength of the solvent, and we assumed that its central tin atom is in a conformationally stable heptacoordinated state.[26]

Table 4. Diffusion Constants (*D*) and the Approximate Spherical Hydrodynamic Radii (*r*) of Methyltin(IV)-Cupferronates in $CDCl_3$ (25 °C, 50 mM for monomers)

compound	D ($\times 10^{-10}$ m^2/s)	r (Å)
$\mathbf{1}_m$	12.08 ± 0.07	3.3 ± 0.1
$\mathbf{2}_m$	9.44 ± 0.04	4.3 ± 0.2
$\mathbf{3}_m$	8.00 ± 0.05	5.0 ± 0.2

Self-Diffusion Behavior and Concentration Dependence. The monomeric nature of solvated methyltin(IV)-cupferronates was further clarified by diffusion ordered spectroscopy (DOSY).[27,28] The apparent diffusion constants were determined by recording the proton 2D-DOSY spectrum for the artificial mixture of all three compounds $\mathbf{1}_t$, $\mathbf{2}_d$, and $\mathbf{3}_m$ (Figure 3). Using the Stokes−Einstein equation[29]

$$D = \frac{k_B T}{6\pi\eta r} \tag{3}$$

the effective hydrodynamic radii (r) were calculated and are listed in Table 4 (k_B is the Boltzmann constant, T is absolute temperature, η is viscosity). These provided structural information about the molecular size of the solvates in a spherical approximation. Increasing the number of bulky Ph(NO)NO− substituents resulted in a stepwise increase in the hydrodynamic radii. Both $\mathbf{1}_t$ and $\mathbf{2}_d$ were bulky assemblies in the solid state, fitting into a sphere with at least 8−10 Å radius. The smaller experimental r values in Table 4, however, reinforced our previous hypothesis that $\mathbf{1}_t$ and $\mathbf{2}_d$ fail to form "stable" self-associated supramolecular complexes in solution at room temperature: they are predominantly monomeric solvates ($\mathbf{1}_m$ and $\mathbf{2}_m$). Combining these results with the geometrical data available in Table 3, the Me−Sn−Me angles suggest that $\mathbf{1}_m$ is dominantly in *cis*-trigonal bipyramidal (*cis*-TBP) conformation, whereas $\mathbf{2}_m$ is in a *cis*-O_h state in dilute solutions of noncoordinating solvents (see Chart 1).

Despite our efforts in observing variations in ^1H, ^{13}C, and ^{119}Sn chemical shifts, any room-temperature con-

(20) Howard, W. F.; Crecely, R. W.; Nelson, W. H. *Inorg. Chem.* **1985**, *24*, 2204−2208.
(21) Manders, W. F.; Lockhart, T. P. *J. Organomet. Chem.* **1985**, *297*, 143−147.
(22) Lockhart, T. P.; Manders, W. F.; Schlemper, E. O. *J. Am. Chem. Soc.* **1985**, *107*, 7451−7453.
(23) Lockhart, T. P.; Manders, W. F. *Inorg. Chem.* **1986**, *25*, 892−895.
(24) Lockhart, T. P.; Davidson, F. *Organometallics* **1987**, *6*, 2471−2478.
(25) Otera, J.; Kawasaki, Y.; Tanaka, T. *Inorg. Chim. Acta* **1967**, *1*, 294−296.
(26) Otera, J.; Hinoishi, T.; Okawara, R. *J. Organomet. Chem.* **1980**, *202*, C93−C94.
(27) Morris, K. F.; Johnson, C. S., Jr. *J. Am. Chem. Soc.* **1992**, *114*, 3139−3141.
(28) Johnson, C. S., Jr. *Prog. Nucl. Magn. Reson.* **1999**, *34*, 203−256.
(29) Edward, J. T. *J. Chem. Educ.* **1970**, *47*, 261−270.

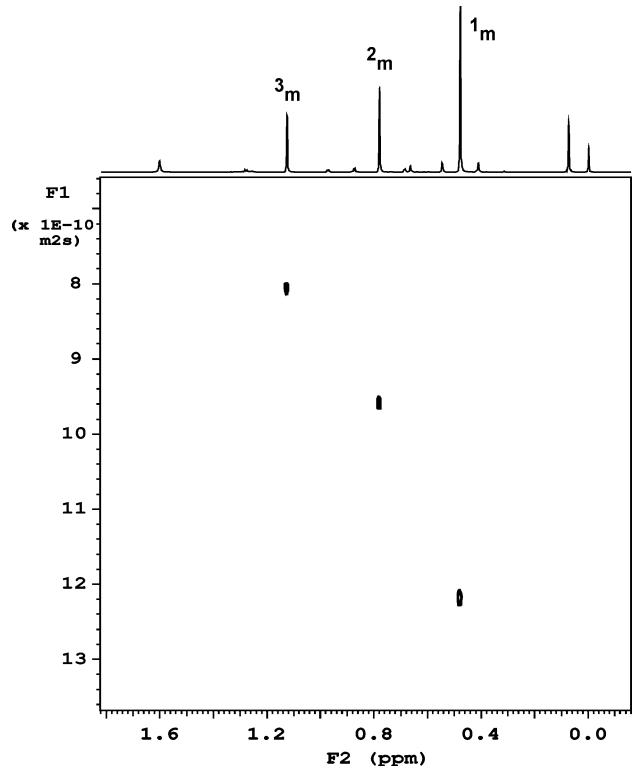

Figure 3. ^{1}H-DOSY-NMR measured for the mixture of methyltin(IV)-cupferronates ($CDCl_3$, 50 mM for the monomers $\mathbf{1}_m$, $\mathbf{2}_m$, and $\mathbf{3}_m$). The horizontal scale represents the ^{1}H dimension (ppm) at the aliphatic region, whereas the vertical scale shows the diffusion scale (m^2/s).

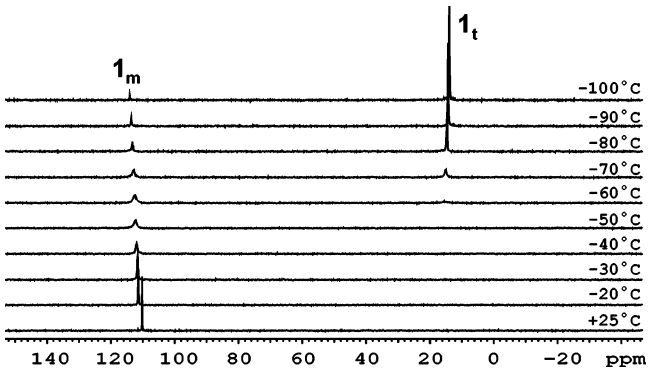

Figure 4. Temperature-dependent ^{119}Sn NMR measurements for $\mathbf{1}_m$ in CD_2Cl_2 at 130 mM concentration.

centration dependent experiment for $\mathbf{2}_m$ in $CDCl_3$ has failed to provide experimental detail for a strong transient self-association behavior. For $\mathbf{1}_m$ some degree of ^{1}H line broadening effects and a less than 10 ppm upfield ^{119}Sn shift were detected in more concentrated solutions (0.5 M or more) in $CDCl_3$.

Observation of the Preorganization Process for $\mathbf{1}_t$. Cooling $\mathbf{1}_m$ in $CDCl_3$ provided clear evidence for the reconstitution of the tetrameric species $\mathbf{1}_t$. To extend the temperature range toward lower values, we replaced $CDCl_3$ with CD_2Cl_2 (Figure 4). At −60 °C and below a sharp resonance appeared significantly upfield to the $\mathbf{1}_m$ signal, indicating a change in the molecular geometry. The upfield shift of the ca. +110 ppm resonance can be rationalized by the *cis*-TBP → *trans*-TBP conformational change associated with the $\mathbf{1}_m \rightarrow \mathbf{1}_t$ transition. The ^{119}Sn chemical shift (+14.3 ppm, −100 °C) of

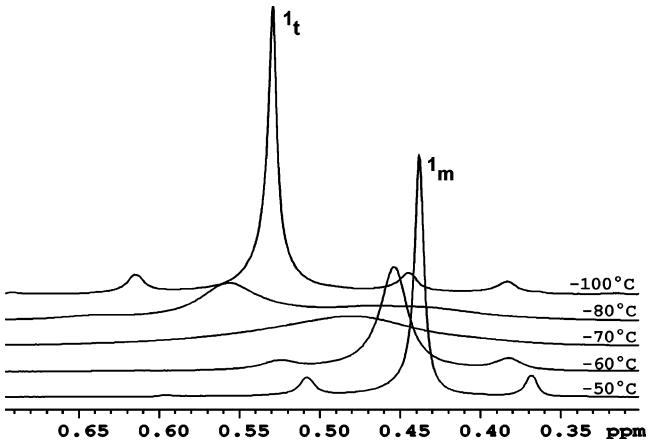

Figure 5. Low-temperature ^{1}H NMR measurements for $\mathbf{1}_m$ in CD_2Cl_2 at 130 mM concentration.

solvated $\mathbf{1}_t$ is rather close to its isotropic shift found earlier in solid-state NMR experiments (−1.5 ppm, +30 °C).[3] Accordingly, Figure 4 shows the first solution evidence for a preorganization process leading to solvated $\mathbf{1}_t$ containing a 20-membered carbon-free metallamacrocycle. We note here that although Gielen et al. have published the solid-state structure of a similar macrocyclic tetramer with a 16-membered $Sn_4C_4O_8$ ring, no spectroscopic data were provided about its dynamics and existence in the solution.[30]

Figure 5 shows a series of low-temperature proton spectra for the 4 $[\mathbf{1}_m] \rightleftharpoons [\mathbf{1}_t]$ equilibrium where the population growth of the ^{1}H NMR signal assigned to $\mathbf{1}_t$ was followed until resharpening of the resonances below the coalescence temperature (ca. −70 °C). The increase in the $|^2J|$ coupling constant seen on the ^{117}Sn/^{119}Sn satellites (from 54.8 to 69.3 Hz) also verifies the $\mathbf{1}_m \rightarrow \mathbf{1}_t$ transition as it corresponds to the 109° → 120° Me−Sn−Me bond-angle variation. Since ^{1}H resonances were exchange broadened, the $|^2J|$ coupling constant for solvated $\mathbf{1}_t$ at −100 °C was determined from the ^{1}H-coupled ^{119}Sn spectra. In contrast to ^{119}Sn NMR, the ^{1}H chemical shift change between the $\mathbf{1}_m$ and $\mathbf{1}_t$ states was rather small (ca. 40 Hz), which rationalizes the fact why room-temperature concentration-dependent chemical shift variations were not indicative of a low-population $\mathbf{1}_t$ (*trans*-TBP) species.

Complexation of $\mathbf{2}_m$ with Lewis Bases. When $\mathbf{2}_m$ was likewise cooled in $CDCl_3/CD_2Cl_2$ solvents, upfield ^{119}Sn shifts were observed, suggesting a higher tin coordination number at low temperatures. In contrast to $\mathbf{1}_m$, however, the ^{119}Sn resonance of $\mathbf{2}_m$ was severely broadened around −230 ppm at temperatures near the freeze-out point of the solute (see Figure S1). Therefore, resharpening of a second ^{119}Sn resonance could not be detected and identification of the solvated supramolecular species $\mathbf{2}_d$ was not possible. Nevertheless, a more shielded ^{119}Sn nucleus was in agreement with a *cis*-O_h → *trans*-O_h conformational change, which is the prerequisite for the homodimerization process leading to $\mathbf{2}_d$ (Chart 1).

By considering all spectroscopic data it seems that $\mathbf{2}_m$ in N- or O-donor Lewis basic solvents is in fast equi-

(30) Gielen, M.; Khloufi, A. E.; Biesemans, M.; Kayser, F.; Willem, R.; Mahieu, B.; Maes, D.; Lisgarten, J. N.; Wyns, L.; Moreira, A.; Chattopadhay, T. K.; Palmer, R. A. *Organometallics* **1994**, *13*, 2849−2854.

Chart 2

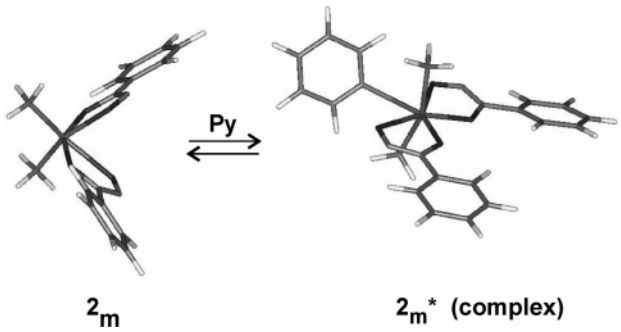

librium between the monomeric hexacoordinated *cis*-O_h and heptacoordinated *trans*-methyl state according to the model for the pyridine complex in Chart 2. In connection to the previously described structural modification of $\mathbf{2}_d$ by pyridine,[3] here we were interested in the determination of the K_a room-temperature equilibrium constant (eq 4) for the above process.

$$K_a = \frac{[\text{complex}]}{[\mathbf{1}_m][\text{Py}]} \tag{4}$$

By the titration of $\mathbf{2}_m$ with pyridine in chloroform we aimed to unravel the origin of the large N-donor-induced ^{119}Sn chemical shifts with the separation of the specificity and the strength of the solute−solvent complexation interaction. Specificity is defined by the ^{119}Sn chemical shift difference between the complexed and uncomplexed species ($\Delta\delta_\infty = |\delta_{complexed} - \delta_{free}|$). When $\Delta\delta_\infty$ is several tens of ppms large, it provides evidence for the change in the tin coordination number and/or conformational change. The magnitude of the association constant (K_a) on the other hand is related to the strength (or stability) of the interaction. As it was pointed out in a previous study,[31] the two parameters ($\Delta\delta_\infty$ and K_a) responsible for the magnitude of the solvent-induced chemical shifts ($|\delta_{obs} - \delta_{free}|$) are independent and their effect is separable. Using the gradient-enhanced version of indirect detection ^{1}H−^{119}Sn-HMQC experiments[32−36] we recorded the ^{119}Sn chemical shifts for $\mathbf{2}_m$ after each pyridine addition (Figure 6). By knowing the total concentration of the dissolved species (c_{2m} for $\mathbf{2}_m$ and c_{py} for pyridine:) the K_a association constant was determined from the δ_{obs} vs c_{py} plot by a well-described nonlinear fitting procedure (Figure 7) using eq 5.

$$\delta_{obs} = \frac{(\delta_{complex} - \delta_{free})(c_{2m} + c_{py} + K_a^{-1} - \sqrt{(c_{2m} + c_{py} + K_a^{-1})^2 - 4c_{2m}c_{py}})}{2c_{2m}} + \delta_{free} \tag{5}$$

where δ_{obs} are the measured ^{119}Sn shifts in the presence of pyridine, whereas δ_{free} is the uncomplexed ^{119}Sn chemical shift for $\mathbf{2}_m$. We found that a relatively small K_a association constant ($K_a = 2.78 \pm 0.02$ L/mol) and a large shift difference ($\Delta\delta_\infty = +215.3$ ppm) were characteristic of this system at room temperature. This allows us to conclude that the above complexation interaction is rather a highly specific than a highly stable one: despite the small stability of the complex large $|\delta_{obs} - \delta_{free}|$ solvent shifts are induced at room temperature due to remarkable changes in the tin geometry. It is worth noting that although the ^{1}H shift variations were not significant in the titrations (Figure

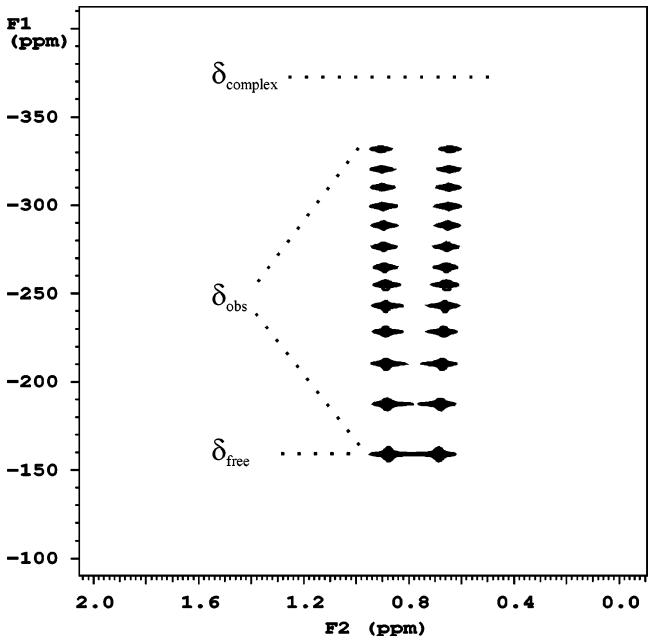

Figure 6. Stack plot of 13 ^{1}H−^{119}Sn-HMQC experiments recorded for $\mathbf{2}_m$ at various pyridine concentrations in a series of titration experiments (c_{2m} = 50 mM, $CDCl_3$, 25 °C). F1 and F2 dimensions represent the ^{119}Sn and ^{1}H chemical shifts, respectively. The pyridine total concentrations (c_{py}) corresponding to the individual titration points are indicated Figure 7.

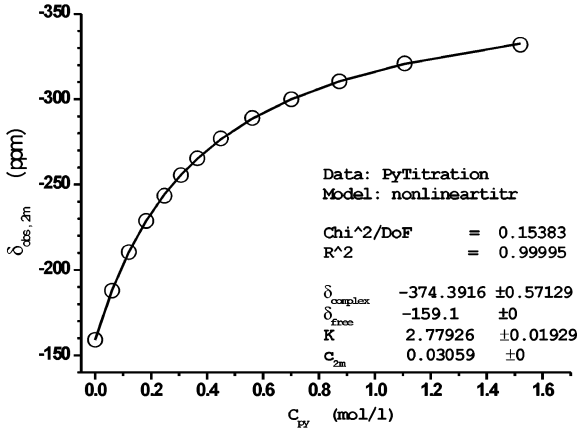

Figure 7. Plot of δ_{obs} as a function of the pyridine total concentration (c_{py}) at constant organotin concentration (c_{2m}). The ^{119}Sn chemical shift values stem from Figure 6 ($CDCl_3$, 25 °C).

(31) Tárkányi, G. *J. Chromatogr. A* **2002**, *961*, 257−276.
(32) Kayser, F.; Biesemans, M.; Boualam, M.; Tiekink, E. R. T.; Khloufi, A. E.; Meunier-Piret, J.; Bouhdid, A.; Jurkschat, K.; Gielen, M.; Willem, R. *Organometallics* **1994**, *13*, 1098−1113.
(33) Willem, R.; Bouhdid, A.; Kayser, F.; Delmotte, A.; Gielen, M.; Martins, J. C.; Biesemans, M.; Mahieu, B.; Tiekink, E. R. T. *Organometallics* **1996**, *15*, 1920−1929.
(34) Willem, R.; Bouhdid, A.; Meddour, A.; Camacho-Camacho, C.; Mercier, F.; Gielen, M.; Biesemans, M.; Ribot, F.; Sanchez, C.; Tiekink, E. R. T. *Organometallics* **1997**, *16*, 4377−4385.
(35) Ribot, F.; Sanchez, C.; Meddour, A.; Gielen, M.; Tiekink, E. R. T.; Biesemans, M.; Willem, R. *J. Organomet. Chem.* **1998**, *552*, 177−186.
(36) Martins, J. C.; Biesemans, M.; Willem, R. *Prog. Nucl. Magn. Reson.* **2000**, *36*, 271−322.

6), $^{1}H-^{119}Sn$-HMQC experiments revealed large ^{119}Sn shift changes, which makes this technique useful for the characterization of weak transient complexes of organotins in dilute solutions. The values $\delta_{complex}$ (−374.4 ppm) and $\Delta\delta_{\infty}$ (+215.3 ppm) determined by nonlinear fitting are also important structural parameters proving a CN = 6 to 7 coordination change around the central tin. Similar titration experiments for diorganotins have not yet been reported in the literature.

Proposed Mechanism of the Dismutation Reaction. Because the solution structures of $\mathbf{1}_m$ and $\mathbf{2}_m$ are now well characterized, we arrive at setting up a proposed mechanism for the dismutation process. The spectroscopic differences for $\mathbf{1}_m$ between measurements in coordinating and noncoordinating solvents (Tables 2 and 3) can be interpreted on the basis of a $\mathbf{1}_m$ (*cis*-TBP) → $\mathbf{1}_m$* (*trans*-TBP) conformational change rather than according to a $\mathbf{1}_m$ (*cis*-TBP) → $\mathbf{1}_t$ (*trans*-TBP) preorganization model. The solute−solute interactions between the monomeric $\mathbf{1}_m$ species, which only dominate at low temperatures in noncoordinating solvents, are replaced by solute−solvent interactions at room temperature in the presence of N- or O-donors in the solvent bulk. As a result, the three methyl carbons of $\mathbf{1}_m$ are pushed by the O- or N-donor solvent (*S*) into a single plane, forcing the cupferronato anion to coordinate (from the opposite direction) rather as a monodendate ligand ($\mathbf{1}_m$* in Chart 1). Similar solvent effects were described for other trimethyltin derivatives with monodendate ligands.[37]

The solvent-perturbed conformational equilibrium for $\mathbf{1}_m$ is the most plausible explanation for the mechanism of the dismutation reaction. Its role is most likely to initiate a process leading to a nucleophilic substitution in which the cupferronato anion is kept in a monodendate transition state whose lifetime is long enough for the proper ligand exchanges to take place via bimolecular collisions. This is in agreement with the fact that the dismutation reaction proceeded at slightly faster rates in DMSO when repeated with lower $[A]_0$ initial concentrations of $\mathbf{1}_m$ ($k = 1.0671 \times 10^{-4} \pm 1.3 \times 10^{-7}$ L·mol^{-1}·s^{-1} at $[A]_0 = 0.110$ mol/l, and $k = 1.6538 \times 10^{-4} \pm 3.7 \times 10^{-7}$ L·mol^{-1}·s^{-1} at $[A]_0 = 0.030$ mol/L, see Table 1). This finding has modified our understanding of the dismutation kinetics, as we previously assumed that a relatively high initial concentration of $\mathbf{1}_m$ is a prerequisite of the transformation. Because titrations have shown that $\mathbf{2}_m$ is stabilized by solvent complexation, we summarize the role of solvent activation according to the following:

$$\mathbf{1}_m \overset{\text{solvent}}{\rightleftharpoons} \mathbf{1}_m^* \qquad \text{(I)}$$

$$\mathbf{1}_m + \mathbf{1}_m^* \rightarrow \mathbf{2}_m^* + Me_4Sn \qquad \text{(II)}$$

$$\mathbf{2}_m^* \overset{\text{solvent}}{\rightleftharpoons} \mathbf{2}_m \qquad \text{(III)}$$

Both solvent-coordinated complexes $\mathbf{1}_m$* and $\mathbf{2}_m$* are abundant because of the omnipresent O- or N-donors in the bulk solvent. Processes I and III are very fast and reversible. The rate-determining step is then process II (as confirmed by the kinetic data), and consequently the order of the reaction remains 2.

(37) Bolles, T. F.; Drago, R. S. *J. Am. Chem. Soc.* **1966**, *88*, 5730−5734.

It is out of the scope of this paper to further describe each contribution that determines the relative rate of the dismutation for the various coordinating solvents (CD_3OD, DMSO-d_6, and C_5D_5N). The fine balance between Lewis basicity, steric, and byproduct (Me_4Sn) solvation factors in methylated solvents (e.g., DMSO) is probably responsible for the fastest reaction rates found in DMSO (Table 1).

Conclusions

We have proven that the supramolecular structures $\mathbf{1}_t$ and $\mathbf{2}_d$ are predominantly monomeric ($\mathbf{1}_m$ and $\mathbf{2}_m$) in solution at room temperature. Both monomeric structures underwent a *cis*−*trans* conformational exchange that is fast on the chemical shift time scales. In noncoordinating solvents ($CDCl_3$, CD_2Cl_2) the dominance of the *cis*-TBP and *cis*-O_h conformations was characteristic for $\mathbf{1}_m$ and $\mathbf{2}_m$, respectively. Coordinating solvents (DMSO, pyridine, and methanol) increased the population of the *trans*-states, increasing the coordination number of the central tins. Solvent-induced conformational change was held responsible for a unique demethylation process in which $\mathbf{1}_m$ was converted into $\mathbf{2}_m$, yielding the byproduct Me_4Sn. Such transformations may explain why no trimethyltin(IV) derivatives of five-membered bidendate anions (cupferronates, kojates, tropolonates) were ever reported as being crystallized from methanol or from other coordinating solvents.

^{1}H NMR kinetic experiments carried out in the spectrometer have proven that the dismutation process followed a second-order 2 A → B + C type kinetics. The rate of the reaction increased with the coordinating strength of the solvent, but the kinetic model has not changed. It seems that the dismutation of $\mathbf{1}_t$ in solution is initiated by intermolecular $\mathbf{1}_m + \mathbf{1}_m$* collisions rather than by intramolecular rearrangements within the supramolecule $\mathbf{1}_t$. The product $\mathbf{2}_m$ was stabilized by the formation of specific heptacoordinated solute−solvent complexes in Lewis base solvents $\mathbf{2}_m$*, which underwent no further dismutation. The underlying *cis*-O_h → *trans*-O_h conformational equilibrium was verified by the calculation of the Me−Sn−Me angles on the basis of *J*-coupling data in the absence and in the presence of O- or N-donor ligands. Additionally, the stability of the solute−solvent complexes of $\mathbf{2}_m$ with pyridine and 4,4′-bipyridyl was characterized by ^{119}Sn NMR titration experiments.

Low-temperature ^{1}H and ^{119}Sn NMR experiments in noncoordinating solvents revealed the first example of a preorganization process toward a solvated 20-membered macrocyclic structure in $\mathbf{1}_t$. The thermodynamic properties of the preorganization process in comparison with those of other triorganotin(IV) derivatives will be published elsewhere.

Compound $\mathbf{3}_m$ prepared as a standard for diffusion experiments showed neither solute−solute or solute−solvent complexation behavior nor spontaneous dismutation reaction in any solvents.

Experimental Section

NMR Experiments. NMR spectra were recorded on a 400 MHz (for ^{1}H) Varian INOVA spectrometer equipped with a Varian 5 mm $^{1}H-^{19}F/\{^{15}N-^{31}P\}$ Z-gradient indirect detection

probe and a direct detection Varian $^{15}N-^{31}P/\{^{1}H-^{19}F\}$ switchable broadband probe (−100 to +150 °C). ^{1}H and ^{13}C chemical shifts are referenced to the residual solvent signals, whereas ^{119}Sn shifts are given relative to the external Me_4Sn (0.00 ppm) signal. 99.95% perdeuterated solvents were purchased from Cambridge Isotope Laboratories. Kinetic experiments were carried out in 5 mm NMR tubes sealed at constriction shortly after dissolution of the crystalline samples. The tube was then inserted in the spectrometer, and the ^{1}H NMR spectra were monitored by setting a 600 s preacquisition delay in an arrayed overnight experiment.

Room-temperature ^{119}Sn chemical shift data were obtained from $^{1}H-^{119}Sn$-gHMQC experiments (for example see Figure S2), while one-dimensional ^{119}Sn was measured at low temperatures. In variable-temperature studies a 20 min preconditioning time was applied before each acquisition. 128 scans were collected for the ^{1}H-decoupled one-dimensional ^{119}Sn spectra with 5 s repetition time. VT gas was cooled by liquid nitrogen. $^{2}J(^{119}Sn-^{1}H)$ coupling constants were determined directly from ^{1}H NMR spectra (Figure S3). Using the method proposed by Kupče and Wrackmeyer et al.[38−41] the $^{1}J(^{119}Sn-^{13}C)$ coupling constants were determined from the ^{119}Sn satellites seen in F1 traces of the gradient-enhanced $^{1}H-^{13}C$-HSQC experiments (2.7 Hz digital resolution) (see Figure S4).

The DOSY experiment was carried out in a 5 mm Shigemi tube ($CDCl_3$ matched) at 25 °C to minimize convection effects. A Performa I. gradient amplifier was used. The gradient strength was calibrated by using 5 w/w% sucrose in D_2O at 25 °C ($D = 5.22 \times 10^{-10}$ m^2/s). The bipolar pulse-pair stimulated echo (Dbppste) sequence was used for acquiring diffusion data with 50 ms diffusion delay, 16 squared increments for gradient levels, and 16 transients. The Varian DOSY package was used for the processing. Chloroform viscosity, $\eta = 5.42$ mPa, was used for the calculation of the hydrodynamic radii at 25 °C.

Titrations were carried out in a 5 mm NMR tube by adding volumes of pyridine solution with a Gilson 50 μL analytical pipet keeping the total organotin concentration constant. The molar ratio of the solutes was followed by accurate ^{1}H integration of the pertinent resonances. $^{1}H-^{119}Sn$-gHMQC experiments were run to obtain ^{119}Sn chemical shift data in 10.5 Hz digital resolution in the F1 dimension. Titration data were plotted and fitted in Microcal Origin 6.1 using a least-squares nonlinear fitting algorithm.

Computational Study. Molecular modeling and geometry optimizations have been performed on a Silicon Graphics Octane computer at the PM3 semiempirical level, employing the MOPAC package in InsightII.

Preparation of Methyltris(*N*-nitroso-*N*-phenylhydroxylaminato)tin(IV) (3_m). The ammonium salt NH_4[PhN(O)NO] (0.70 g, 4.5 mmol) dissolved in 15 mL of distilled water was added to a solution of $MeSnCl_3$ (0.36 g, 1.5 mmol) in 5 mL of distilled water. Precipitation of the complex occurred immediately. After stirring for 15 min at room temperature the precipitate was filtered off and washed with cold distilled water and dried in air. The complex is hygroscopic and, after few weeks of standing, converted into monohydrated material according to ^{1}H NMR ($CDCl_3$, 25 °C). Yield: 0.73 g, 89%. Mp: 79−80 °C. FT-IR (KBr): ν 3432 cm^{-1} (O−H) (w b), 3105−2921 (w b), 1591 (O−H) (w), 1486 (Ph) (m), 1463 (Ph) (ms), 1347 (N−N) (ms), 1295 (vs), 1224 (N=O) (ms), 1184 (N=O) (ms), 1165 (ms), 1066 (ms), 1022 (m), 937 (ONNO) (s), 926 (ms sh), 756 (Ph) (s), 694 (Ph) (s), 683 (OSnO) (s sh), 617 (w), 600 (sh), 573 (w b), 505 (w), 401(Sn−O) (vs). ^{1}H NMR (399.89 MHz, CDCl3): δ 1.12 (s, $^{2}J(^{117}Sn/^{119}Sn-^{1}H) = 120.1/125.3$ Hz, 3H, CH_3); 1.55 (s, 2H, H_2O); 7.43−7.50 (m, 9H, CH); 7.92−8.00 (m, 6H, CH). ^{13}C NMR (100.56 MHz, $CDCl_3$): δ 7.3 (s, $^{1}J(^{117}Sn/^{119}Sn-^{13}C) = 1123/1178$ Hz, CH_3); 119.8 (s, CH); 129.2 (s, CH); 130.5 (s, CH); 139.6 (s, C). ^{119}Sn NMR (149.08 MHz, $CDCl_3$): δ −478.6 ppm. Anal. Calcd for anhydrous $\mathbf{3}_m$ $C_{19}H_{18}N_6O_6Sn$ (545.10): C, 41.9; H, 3.3; N, 15.4. Found: C, 41.9; H, 3.5; N, 15.4.

Acknowledgment. The authors would like to thank Dr. Péter Sándor (Varian Deutschland Gmbh) for NMR application support. We thank the Hungarian Research Fund (OTKA) Grant T047321 for supporting the work.

Supporting Information Available: Four figures showing details of NMR experiments. This material is available free of charge via the Internet at http://pubs.acs.org

OM050279Y

(38) Kupče, Ē.; Wrackmeyer, B.; Granger, P. *J. Magn. Reson.* **1969**, *100*, 401−405.
(39) Wrackmeyer, B.; Kupče, Ē.; Kümmerlen, J. *Magn. Reson. Chem.* **1992**, *30*, 403−407.
(40) Wrackmeyer, B.; Kupče, Ē.; Kehr, G.; Sebald, A. *Magn. Reson. Chem.* **1992**, *30*, 964−968.
(41) Wrackmeyer, B.; Horchler von Locquenghien, K.; Kupče, Ē.; Sebald, A. *Magn. Reson. Chem.* **1993**, *31*, 45−50.